AD866344

AD No.
DDC FILE COPY

NAVAL ORDNANCE LABORATORY
LIBRARY

[redacted]

(18) NAVORD ~~REPORT~~ 3968 (17)

AUG

(6) THE DETONATION PRESSURES IN EXPLOSIVES AS MEASURED BY TRANSMITTED SHOCKS IN WATER,

(10) William C. Holton

CLEARED
FOR OPEN PUBLICATION
24 FEB 1970
Chief of Naval Material (PA)

(11) 1 DEC [redacted] 54

[redacted]

(12) 26p.

1st Edition ED 1948
1 September 1960

(16) NOL-Bec-1-1-55

U. S. NAVAL ORDNANCE LABORATORY

WHITE OAK, MARYLAND

DDC

Best Available Copy

Un-

This document is CLASSIFIED and shall be safeguarded in accordance with the security provisions of U. S. Navy Regulations. It is forbidden to make extracts from or to copy this classified document without specific approval of the Chief of Naval Operations or originator, as applicable, except as provided for in article 9-10 of the United States Navy Security Manual of Classified Matter.

Unclassified
~~CONFIDENTIAL~~

NAVORD Report 3968

THE DETONATION PRESSURES IN EXPLOSIVES AS MEASURED BY TRANSMITTED SHOCKS IN WATER

by:

WILLIAM C. HOLTON

Approved: S. J. Jacobs
Chief, Detonation Division

ABSTRACT: A method is described for observing the first twenty-five millimeters of travel of the underwater shock wave propagated at the end of small cylindrical explosive charges. A suitable theory is developed to allow a simple computation of the explosive detonation pressure from these observations. The feasibility of mapping the pressure contour of the explosive by this method is considered.

page i

EXPLOSIVES RESEARCH DEPARTMENT
U. S. NAVAL ORDNANCE LABORATORY

Unclassified
~~CONFIDENTIAL~~

NAVORD Report 3908 1 December 1954

The work described herein was conducted in the Detonation Division under project No. NOL-B2c-1-1-55. It is part of an investigation which is intended to study detonation properties by quantitative observations of the underwater shock wave produced by the detonation of explosives. While considered valid and informative, the results are not considered a basis for action.

JOHN T. HAYWARD
Captain, USN
Commander

Paul M Fye

PAUL M. FYE
By direction

CONTENTS

ABSTRACT . . . . [illegible]

INTRODUCTION . . . . [illegible]

HYDRODYNAMIC PROBLEM . . . . [illegible]

EXPERIMENTAL TECHNIQUE . . . . [illegible]

EXPERIMENTAL RESULTS 6

CONCLUSIONS 7

ACKNOWLEDGEMENTS 11

REFERENCES 21

TABLES AND ILLUSTRATIONS

TABLE I. TNT/Al Pressure Analysis 8

TABLE II. RDX/Al Pressure Analysis 9

TABLE III. TNETB/Al Pressure Analysis 10

FIGURE I. Experimental Apparatus 12

FIGURE II. Terminal Shock Wave Velocity in Water 13

FIGURE III. Variation of $\log_{10}$ Shock Velocity with Distance From Lower Surface of Charge for 80/20 RDX/Al 14

FIGURE IV. Variation of $\log_{10}$ Shock Velocity with Distance From Lower Surface of Charge as a Function of Aluminized RDX Composition 15

FIGURE V. Variation of $\log_{10}$ Shock Velocity with Distance From Lower Surface of Charge as a Function of Aluminized TNETB Composition 16

FIGURE VI. Underwater Initial Shock Pressures of TNETB/Al and RDX/Al as a Function of the Percent Aluminum 17

FIGURE VII. Detonation Pressures of TNETB/Al and RDX/Al as a Function of the Percent Aluminum 18

FIGURE VIII. Values of the Adiabatic Exponent for RDX/Al and TNETB/Al as a Function of the Percent of Aluminum . . . 19

FIGURE IX. Variation of the Logarithm of the Underwater Shock Pressure with the Reciprocal of the Underwater Shock Velocity. . 20

THE DETONATION PRESSURES IN EXPLOSIVES AS MEASURED BY TRANSMITTED SHOCKS IN WATER

INTRODUCTION

The determination of pressures in a detonating explosive when the pressure discontinuity is as high as 300 kilobars and the transient time on the order of several microseconds is best attempted by the measurement of some variable of the system other than the pressure. Two approximate methods of this type based on shock velocities in metals and Taylor's expanding case theory are described in reference (5). A rigorous method for which the density of the product gases is determined has been described in reference (6).

The velocity and rate of decay of a shock wave propagated into water at the end of a two inch diameter by four inch length plane wave initiated explosive charge has been observed using a rotating mirror camera shadowgraph technique. The photographic records obtained are read on a microcomparator as displacement versus time curves, and a quadratic equation fitted by the method of least squares. The velocity of the water shock is obtained as a function of time or distance from the first differential. From the measurement of the initial velocity of the water shock, an extrapolation to the higher shock pressure data presented by Snay and Rosenbaum in NAVORD 2383, reference (1), is possible. This information plus hydrodynamic theory permits a calculation of detonation pressures and values of the adiabatic exponent, if the relationship between detonation velocity and explosive loading density is known.

Approximate detonation pressures may also be calculated from the condition of impedance mismatch, reference (3). Pressures calculated by this method are in good agreement with those obtained by the preceeding method. It would appear therefore that the water shock is a "good" reflection of the pressure profile in the detonating explosive.

By a method of obtaining tangents at random points of the photographic record, a direct plot of the underwater shock velocity versus distance into the water is available. A linear equation is fitted by the method of least squares to the data of $\log_{10}$ Shock Velocity versus distance into the water over the range, 2.5 millimeters to 16.0 millimeters. This equation is extrapolated to zero distance to obtain the initial underwater shock velocity. Detonation pressures may then be calculated by the preceeding methods.

HYDRODYNAMIC PROBLEM

The extrapolation of the data presented in NAVORD 2383 in reference (1) entitled "Shock Wave Parameters in Fresh Water for Pressures Up to 95 Kilobars", has been made in the form:

$$(1)\quad \log_{10} P_w = f\left(1/D_w\right) = 3.067 - 5287 \cdot \frac{1}{D_w}$$

This permits a determination of the pressure and particle velocity immediately behind the water shock front. The form of the extrapolation has been chosen as a straight line function, see Figure IX.

The following notions of the hydrodynamic problem of the explosive at the explosive-water interface permit the development of a simple hydrodynamic theory suitable for the calculation of the approximate detonation pressure, reference (3), from the measurement of the initial underwater shock velocity, a knowledge of the detonation velocity versus loading density curves, and the data of Snay and Rosenbaum for water. The fundamental hydrodynamic equations relating front velocity, D, and material velocity, u, to the detonation pressure, P, and density, ρ, are:

$$(2)\quad \frac{D_e - u_e}{D_e} = \frac{\rho_o}{\rho_e}$$

$$(3)\quad P_e = D_e u_e \rho_o$$

where the subscript "e" refers to reacted explosive and the subscript "o" refers to unreacted explosive. At the detonation front, the Chapman-Jouguet condition applies.

$$(4)\quad C_e = D_e - u_e$$

When the detonation reaches a boundary, e.g., water, an expansion occurs in the gases, and the water is assumed to be compressed in a square step shock. The gas expansion satisfies the non-steady state one dimensional conditions treated by Riemann. If u' is the particle velocity of the gases after an isentropic expansion to the pressure equal to that transmitted into the water, then:

$$(5)\quad u' - u_e = -\int \frac{c}{\rho}\, d\rho$$

The sound velocity, C, is related to P and ρ by the expression,

$$(6)\quad c^2 = \left(\frac{\partial P}{\partial \rho}\right)_S$$

so that the above integral can be evaluated if P is known as a function of ρ at constant entropy. We will assume

(7) $P = A_{(s)} \rho^{\kappa}$

where "A" and "kappa", the exponent are constant at ... the explosive-water interface, U' equals ... From ... with appropriate substitutions, we may derive the relation

(8) $U_w = \frac{D_e}{\kappa + 1} + \frac{2\kappa D_e}{\kappa^2 - 1} \left\{ \ldots \left[\frac{P_w}{\rho_{1e} D_e^2} \ldots \right] \right\}$

and (9) $P_e = \frac{D_e^2 \rho_e}{\kappa + 1}$

In expression (8) U_w, D_e, P_w, and ρ_e are known so that ... can be determined. This value when used in (9) gives the detonation pressure.

A second approach to the solution of the hydrodynamic problem at the explosive-water interface is possible if the momentum equation for strong shock waves is considered.

(3) $P = D u \rho_0$

It may be assumed as was previously done that the water is compressed in a square step shock, and the Chapman-Jouguet condition applies to the explosion products. The problem resolves itself to one of solving the boundary conditions for a square step shock incident on the boundary between two media, each of which may have a different shock impedance, reference (3). The detonation pressure is then expressed in the relations:

(10) $P_e = P_w \left[\rho_w D_w + \rho_e D_e\right] / 2 \rho_w D_w$

where the subscripts "e" and "w" refer respectively to explosive and water. This relation is realized to be only an approximation as the wave reflected from the interface is a rarefaction, whereas to conform with theory it should be a weak shock. This approximation appears at first to be intolerable. The results obtained with this expression however, are in good agreement with those obtained from the preceeding method.

EXPERIMENTAL TECHNIQUE

The first one inch of travel of the shock wave propagated into distilled water at the end of a plane-wave initiated explosive charge has been observed for TNT/Al, and RDX/Al charges with the percentage of aluminum by weight ranging from 0% to 60% in 10% increments. This has been accomplished through the use of a rotating mirror camera employing a shadow-graph technique. The explosive charges with the exception of TNT/Al were made of four stacked two inches diameter by one inch height pressed pellets. The TNT/Al charges were cast cylinders two inches in

diameter by four inches height. The entire ex[illegible] of a Hercules Special detonator, a two [illegible] of the pentolite-baratol type, a tetryl [illegible] one inch in height, and the explosive [illegible] lower face of each charge was examined f[illegible] firing, and only charges wit[illegible] were used. Because the charge was to [illegible] mately five minutes before being detonated, all [illegible] were previously tested for water a[illegible]tion. [illegible] water absorbed in this length of time was negligible.

The position of the explosive charge and optical components [illegible] inside the bombproof are shown in Figure I. Wooden aquari[illegible] by 7" serve as containers for the distilled water in which the charge is detonated. The two opposite larger sides are made of a good grade of window glass to allow an undistorted view of the event. On the outside of the rear glass wall is mounted an 11" focal length lens which focuses the light from the shadow-gram light source on the front lens of the rotating mirror camera. The light source, lens, and acquarium are aligned along the optical axis of the rotating mirror camera, with this optical axis perpendicular to the glass surfaces of the acquarium. The light source is an exploding tungsten wire one mil in diameter, threaded through a capilliary tube 3" in length by one millimeter inside diameter. This wire is pulsed with 4000 volts approximately 15 microseconds before the detonation front reaches the lower end of the explosive train. The capilliary tube of the light source is placed parallel to the lower surface of the explosive charge, i.e., in the horizontal plane, with its center on the optical axis of the system. With the light source in this position there is effectively in the vertical plane, a point source of light which is focused on the front lens of the rotating mirror camera. This arrangement avoids distortion due to parallax reflections from the front surface of the under-water shock wave. The explosive charge is immersed in the filled aquarium to a depth of 2.25 inches. In this position the lower surface of the charge is horizontal, and 0.5 inches above the optical axis of the combined camera-light source system. Furthermore, the charge is positioned so that its extended axis intercepts the optical axis of the system. The rotating mirror camera is then critically focused on the extended axis of the explosive charge.

To increase the image resolution, the usual one and a half inch thick plexiglass viewing window in the bombproof wall has been replaced with series of one inch thick steel plates in which 0.3 inch width slots hav been cut (see Figure I). These plates are positioned with air gaps in between to reduce the blast effect at the camera to such a degree that only a 0.25 inch thick plexiglass slab is necessary immediately in front of the objective lens of the camera to stop material from the explosion from striking the objective lens. The 0.25 inch plexiglass window in this position does not introduce a detectible distortion of the image.

The rotating mirror camera and associated controls for synchronizing the exploding wire light source and time of detonation of the charge with the position of the mirror are described below. The streak photograph picture is taken on 35 mm. film at a known image velocity and a known reduction in magnification. In these photographs of which Figure 1 is an example, vertical displacement on the film corresponds to linear displacement along a narrow line through the extended axis of the charge as seen by the camera. Horizontal displacement on the film corresponds to time. The film drum is so positioned in relation to the rotating mirror that the magnification is constant over the length of the drum used in making the records. Prior to each shot the magnification is measured by photographing a precision scale which is placed in the position where the center of the charge will be. Photographs are also taken of the image of the vertical slit on the film drum to determine its tilt from the vertical. These pictures are made at two positions on the film drum since the geometry of the camera requires the image of the slit to change its tilt as it is swept down the length of the film drum by the rotating mirror. A "slit tilt" correction is therefore applied to the position of the smear photograph. The geometry of the camera also requires that the image velocity along the film drum for a given mirror rotation speed be a function of the distance of the image from a known position of the film drum. This time calibration has been obtained for a mirror rotation speed of 600 rps. The method consisted of photographing light pulses emitted by a high speed light pulser, reference (4), while accurately noting the position of the film on the film drum. Succeeding films are then positioned to within 0.1 mm. of the calibration film. The rotational speed of the mirror during any experiment with the camera is determined in the following manner. Timing signals generated at each revolution of the mirror are impressed on the y-axis of an oscillograph screen. A sine wave is impressed on the x-axis from a 100 cycle per second tuning fork. The inherent accuracy of the fork is 0.01 cycle per 100 cycles. The mirror speed can be determined in multiples of 100 revolutions per second. The additional errors involved are functions of mirror speed and operator technique. If the operator allowed the oscillograph pattern to drift one cycle in ten seconds, at a mirror speed of 600 rps, he would make an error of 0.02%. The density variation within a single aluminized charge is estimated to be 0.3%. The overall estimate of the precision of the velocities measured is about 0.5%.

The relative humidity and temperature of the film chamber of the rotating mirror camera are maintained at fairly constant values. The films are developed immediately after exposing for eight minutes in

Kodak D-11 developer at 68°F, and fixed for fifteen minutes in acid hypo at 68°F. After washing and drying the films are stored between heavy sheets of glass. The measureable film lengthwise shrinkage in this process is negligible.

The photographic records are read on a Gaertner micro-comparator to obtain displacement versus time curves. Referring to Figure II, the line AB is aligned parallel to the horizontal movement of the micro-comparator. Vertical measurements (displacement) are made using equal increments of the horizontal movement (time). Both the horizontal and vertical movements of the micro-comparator are accurate to 0.001 millimeter. To obtain a velocity versus distance curve, tangents to the curve at identifiable points on the curve are measured on the micro-comparator, which is accurate to 0.01° of angular measure. Points along the curve are identified by placing a ruled grid with one millimeter spacing between parallel lines over the record on the table of the comparator. The intersection of the ruled lines with the curve identify the points at which the tangent is to be measured. The distance of each point from the lower face of the charge is obtained by aligning the line AB (see Figure II) with the horizontal movement of the comparator, and making measurements to the point with the vertical movement. The field of view and magnification of the comparator are adjusted such that when using the entire field of view for fitting the tangent at a given point, the trailing edge of this field of view forms the center of the following field of view when fitting the tangent to the curve at the adjacent point.

The angle between the slits, lines marked CE and another not shown and the line marked AB in Figure II is measured. The change in slit tilt between the two positions of the photographed slits is determined, and the rate of change computed assuming it to be linear. A "slit tilt" correction is thereby applied to the measured points and tangents along the shock front curve. The magnification is measured from the film and the image velocity determined from the known position of the image on the film drum. The average magnification of this series is approximately 1.6?, and the average image velocity is approximately 1.31 mm/microsecond.

EXPERIMENTAL RESULTS

The explosive compositions that have been investigated in the preceeding manner are TNT/Al, TNETB/Al, and RDX/Al. The TNT/Al charges were fired for comparative purposes and to develop the experimental technique required to obtain the displacement versus time curves. Since several experimental modifications have been made both during and after these charges were fired, it is felt that the results obtained are not as reliable as the later work done on RDX/Al and TNETB/Al. A summary of the explosive parameters obtained for TNT/Al is presented in Table I. The

initial underwater shock velocity was obtained by analyzing the record to obtain a displacement versus time curve to which was fitted a quadratic equation by the method of least squares. The first difference at time zero produces the initial underwater shock velocity. Pressure calculations have been made both from the theory previously presented and from the conditions of impedance mismatch.

A summary of the explosive parameters obtained for TNETB/Al and RDX/Al is presented in Table II and Table III respectively. The initial underwater shock velocities for these compositions were obtained as follows. Referring to Figure III, which shows the analysis of RDX/Al (80/20), the logarithm of the shock velocity calculated from readings of the shock velocity at arbitrary distances from the lower surface of the charge on the photographic record by the method of tangents to the curve, is plotted as a function of the distance from the lower surface of the charge for all the charges of this composition that were fired. The vector mean of each set of points (see small box of Figure III) is taken to obtain the broken line curve. The error introduced in this calculation is negligible since the maximum angle between any two raw data curves at any one point is less than 5°. A straight line is then fitted by the method of least squares to the broken line curve. This calculation is carried out from 2 millimeters distance to 16 millimeters distance (see large box of Figure III) and extrapolated to zero distance. This is justified since considerable spread is introduced into the data near both ends of the photographic record. Figures IV and V present the least square curve obtained for varying compositions of RDX/Al and TNETB/Al respectively. Pressure calculations have been made both from the theory previously presented and from the conditions of impedance mismatch.

CONCLUSIONS

The initial underwater pressure, the detonation pressure, and "kappa" values for RDX/Al and TNETB/Al compositions are plotted as a function of the percent aluminum in Figures VI, VII, and VIII, respectively. The data for the 60/40 RDX/TNT composition is possibly incorrect in that the initial underwater shock velocity resulting from this composition is slightly higher than that from 70/30 RDX/Al. Omitting this value it is seen that the detonation pressure decreases as the percent aluminum is increased from 10% to 50% within the experimental error. The slope of the detonation pressure vs % Al curve for the TNETB/Al compositions is less steep than that of the RDX/Al mixtures. If the data for 60/40 RDX/Al is disregarded, the magnitude of "kappa" increases with aluminum addition to TNETB, but rises to a maximum at approximately 30% aluminum for RDX and then falls. Referring to the curves of the $\log_{10}$ Shock Velocity as a function of the distance into the water from the lower surface of the charge, the explosive composition of RDX/Al which is most effective in

TABLE I

TNT/Al Pressure Analysis

% Al	No. of Shots	Density	% Theor. Density	Detonation Velocity	Shock Velocity	Γ_w	P_e(IM)	P_e(equ)	U_*	Kappa
0	4	1.660	96.7	6740	5270	117	178	[illegible]	[illegible]	[illegible]
21.7	4	1.769	98.0	6770	5260	118	[illegible]	[illegible]	[illegible]	3.3
[illegible]	4	1.933	98.6	6655	5040	105	[illegible]	182	[illegible]	3.7
61.2	4	2.093	96.5	6140	4440	75	148	138	[illegible]	[illegible]

Units: Pressures, kilobars
Densities, gm/cc
Velocities, m/sec

TABLE II

RDX/Al Pressure Analysis

%Al	No. of Shots	Density	% Theor. Density	Detonation Velocity	Shock Velocity	P_{H2O}	P_e(IM)	P_e(equ)	U_w	Kappa
0	3	1.641 ±.002	91.1	8300	6500 ± 30	178.2	275.8	269	2742	3.2
10	3	1.680 ±.001	90.3	8030	6030 ± 20	154.9	250.7	246	2569	3.4
20	6	1.729 ±.002	89.6	7770	5720 ± 20	139.0	232.7	227	2430	3.5
30	3	1.794 ±.002	89.5	7580	5470 ± 40	125.9	219.5	210	2302	3.9
40	2	1.835 ±0	88.5	7200	5500 ± 80	127.4	216.7	211	2316	3.5
50	2	1.888 ±.003	87.5	6810	5240 ± 70	114.0	196.9	190	2176	3.6

TABLE III

TNETB/Al Pressure Analysis

%Al	No. of Shots	Density	% Theor. Density	Detonation Velocity	Shock Velocity	P_{H2O}	P_e(IM)	P_e(equ)	U_w	Kappa
0	3	1.688 ±.006	94.9	8120	6380 ± 30	172.6	272	265	2705	3.2
10	2	1.750 ±.002	95.1	8120	6240 ± 50	164.4	269	262	2635	3.4
20	3	1.823 ±.008	95.3	7990	5860 ± 30	145.5	254	248	2433	3.7
30	3	1.880 ±.006	95.0	7840	5470 ± 40	125.9	233	227	2302	4.1
40	3	1.948 ±.002	94.7	7590	5200 ± 40	112.2	216	208	2155	4.4

maintaining a high underwater velocity is that obtained with the addition of 30% aluminum. In aluminized TNETB similar results are obtained ... 40% Al.

The experimental technique employed for the observation of underwater shock waves as a function of time affords an excellent method for the mapping of the pressure contour of an explosive. The time resolution of the rotating mirror camera used in these experiments was not sufficiently accurate to observe small regions of the shock velocity versus time curve. The best fit to the experimental data obtained was therefore the straight line used. There are indications however, that though a constant shock velocity may exist over the first few millimeters of shock travel a sharp fall in the shock velocity follows. At the present time, a faster rotating mirror camera is under construction. When completed it will permit this event to be observed in greater detail.

ACKNOWLEDGEMENTS

The author wishes to thank Dr. S. J. Jacobs who suggested the method of applying the hydrodynamic theory presented in this report, and who has supplied valuable advise and criticism in this work. The cooperation of T. P. Liddiard in offering many useful suggestions; and the work of Malcom Curtis and D. J. Danielson in carrying the project to completion is appreciated.

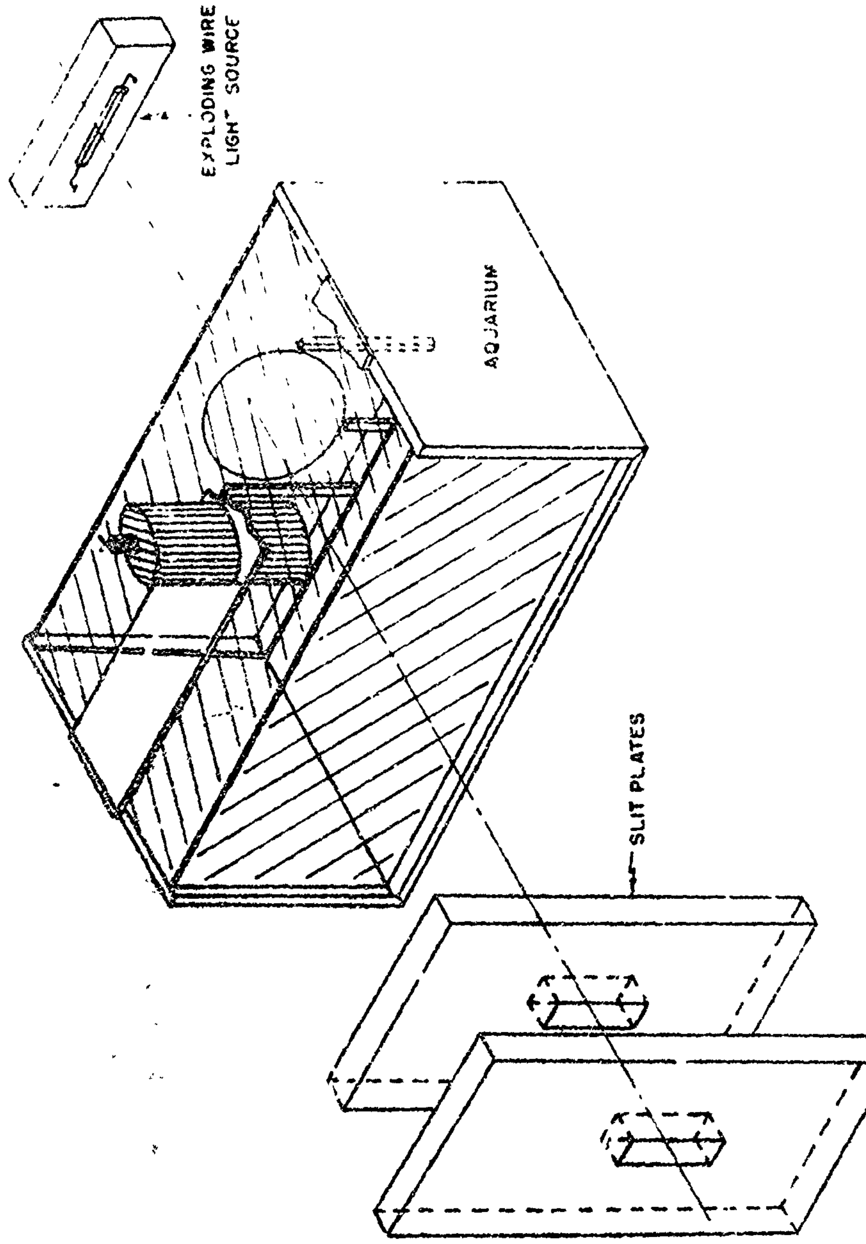

FIG.1 EXPERIMENTAL APPARATUS

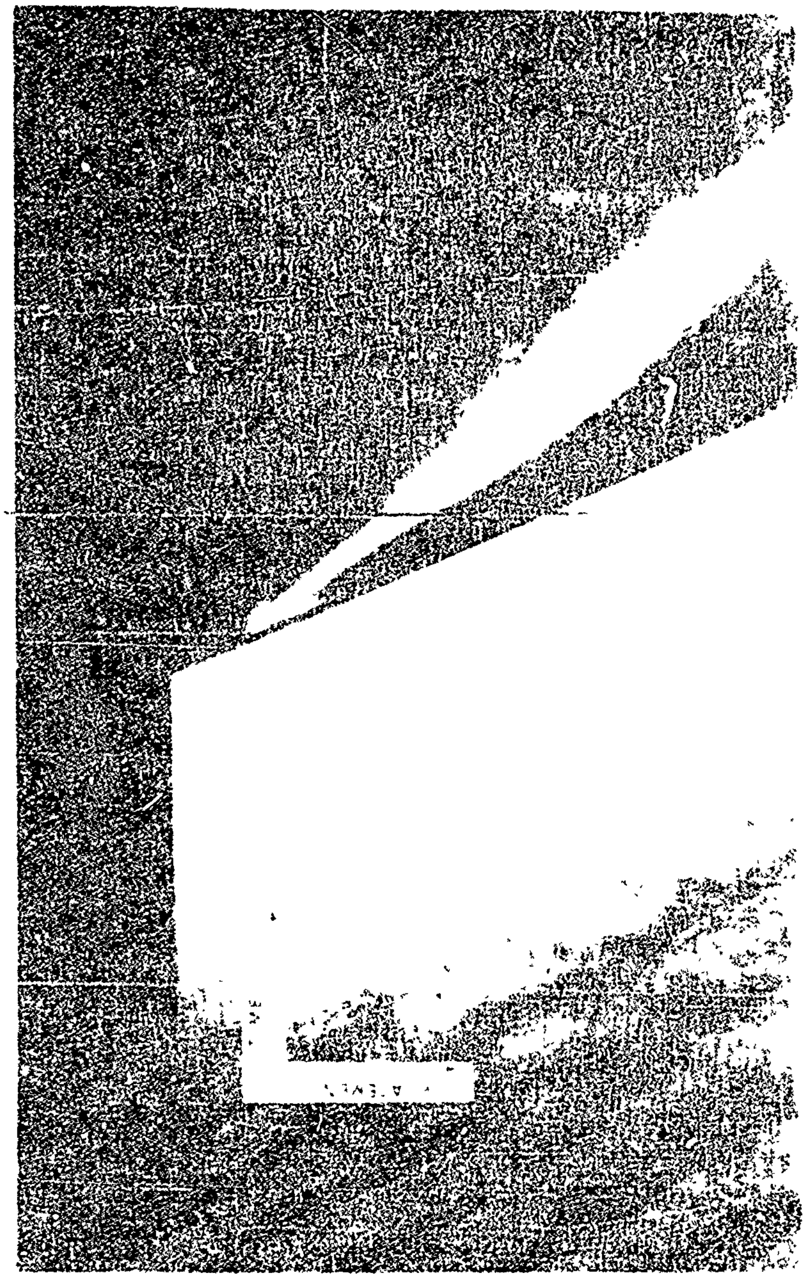

CONFIDENTIAL

Unclassified

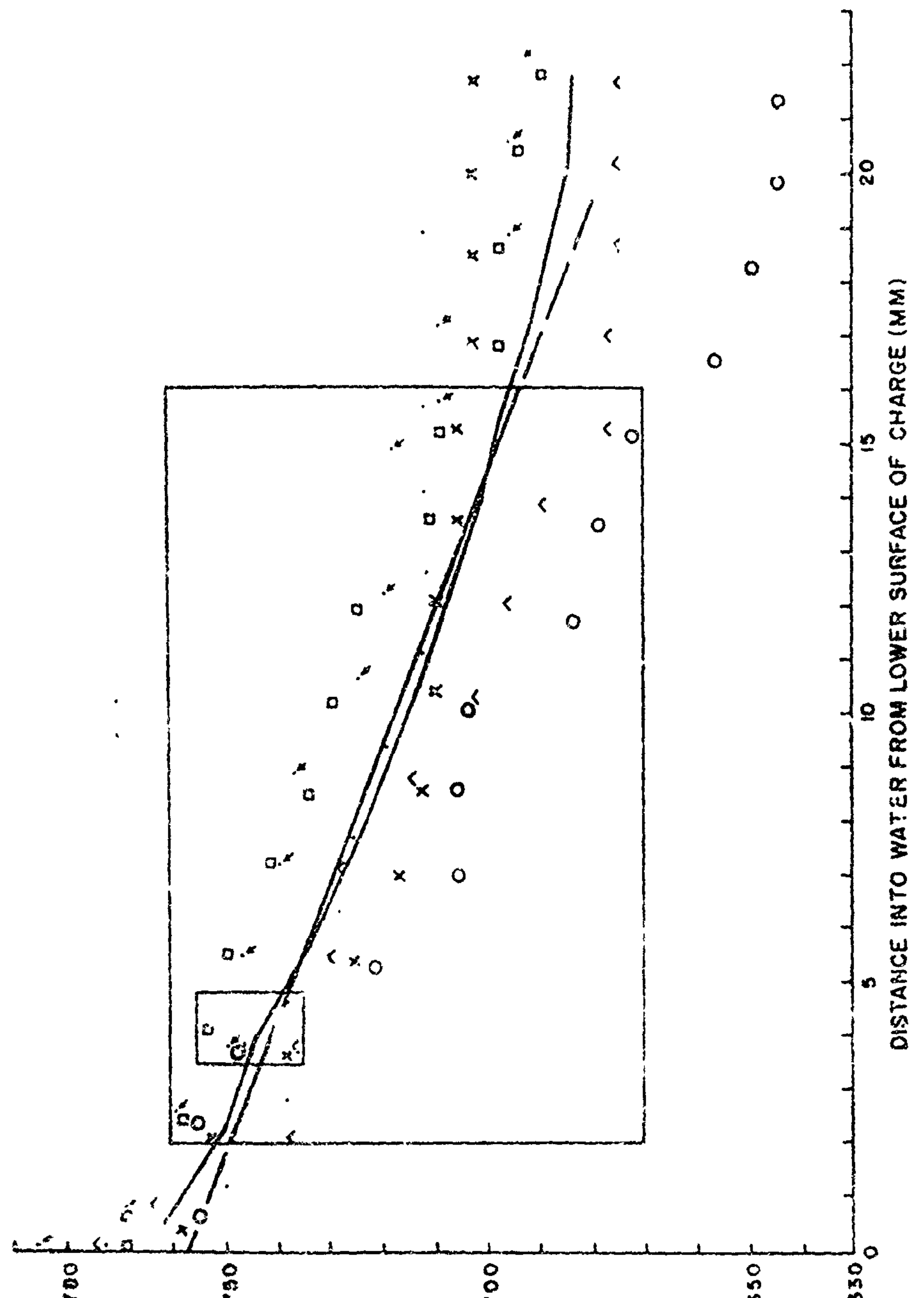

FIG.3 RDX/Al (80/20) LOG_{10} SHOCK VELOCITY = 0.757 − 0.004 (DIST)
MEAN DEVIATION OF MEAN = ± 0.002

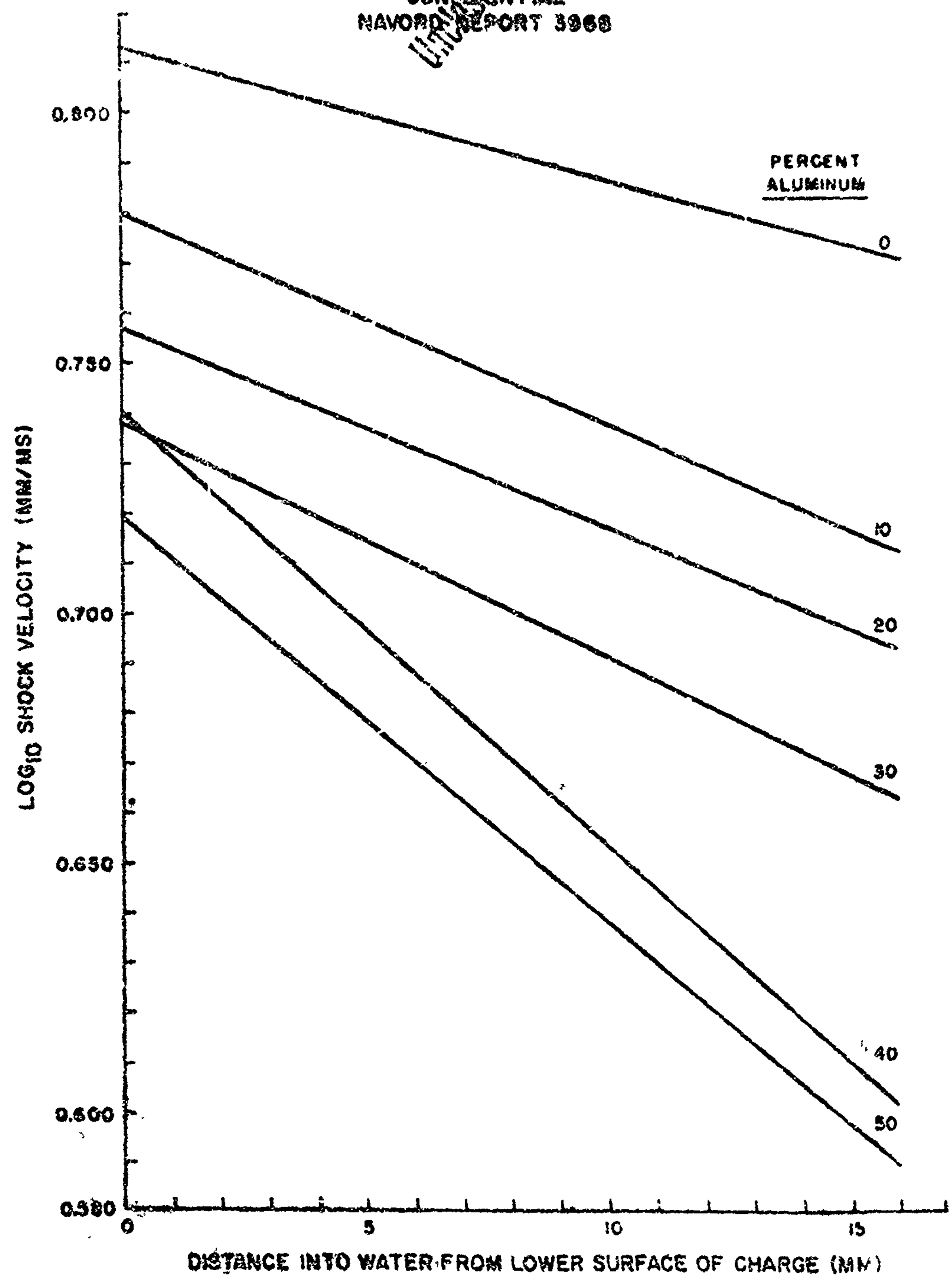

FIG. 4 RDX/Al LOG$_{10}$ SHOCK VELOCITY AS A FUNCTION OF DISTANCE INTO WATER FROM LOWER SURFACE OF CHARGE

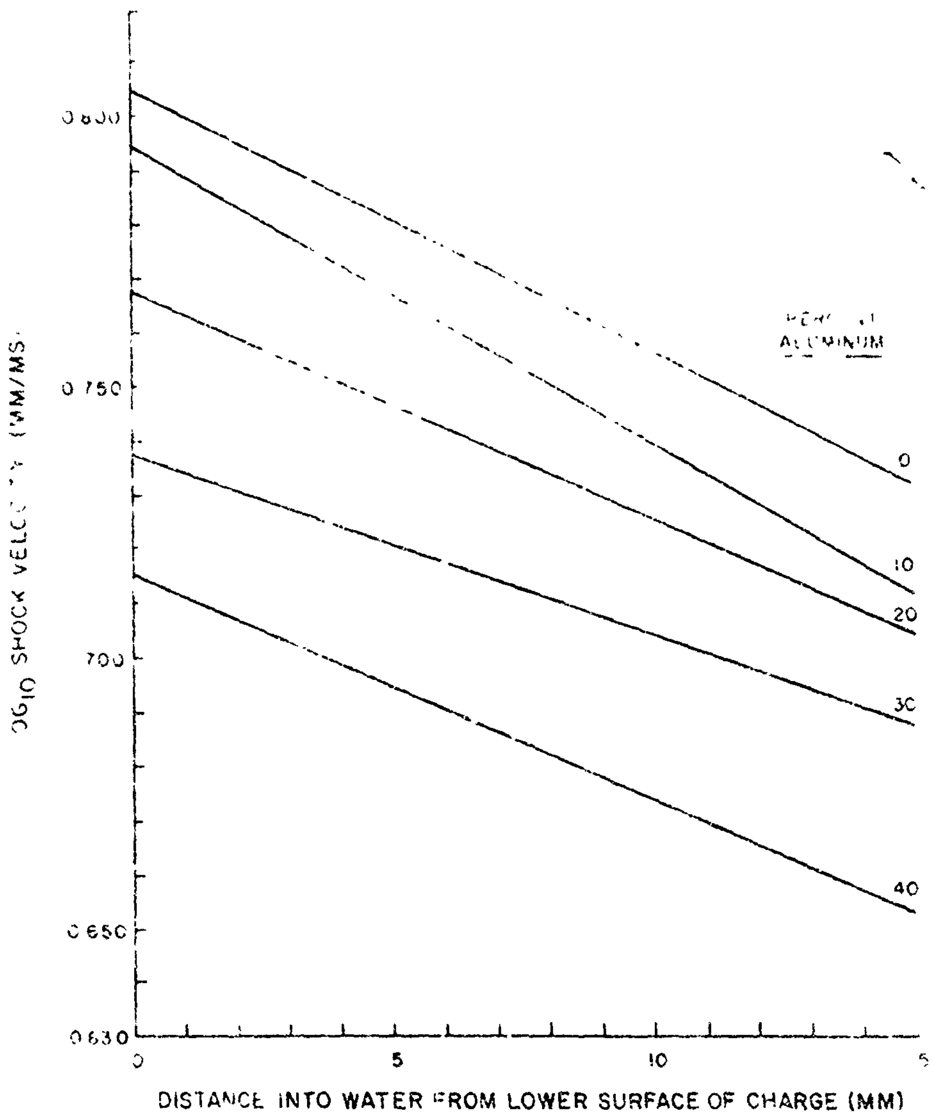

FIG. 5 TNETB/Al LOG$_{10}$ SHOCK VELOCITY AS A FUNCTION OF DISTANCE INTO WATER FROM LOWER SURFACE OF CHARGE

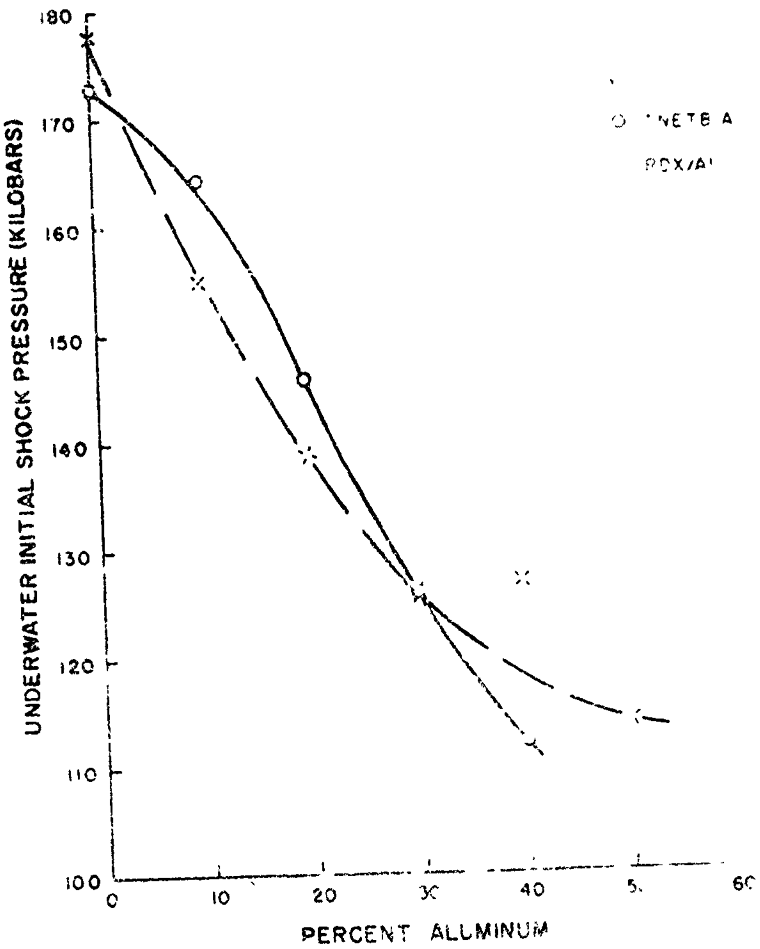

FIG. 6 UNDERWATER INITIAL SHOCK PRESSURES OF ... AND RDX/Al AS A FUNCTION OF THE PERCENT ALUMINUM

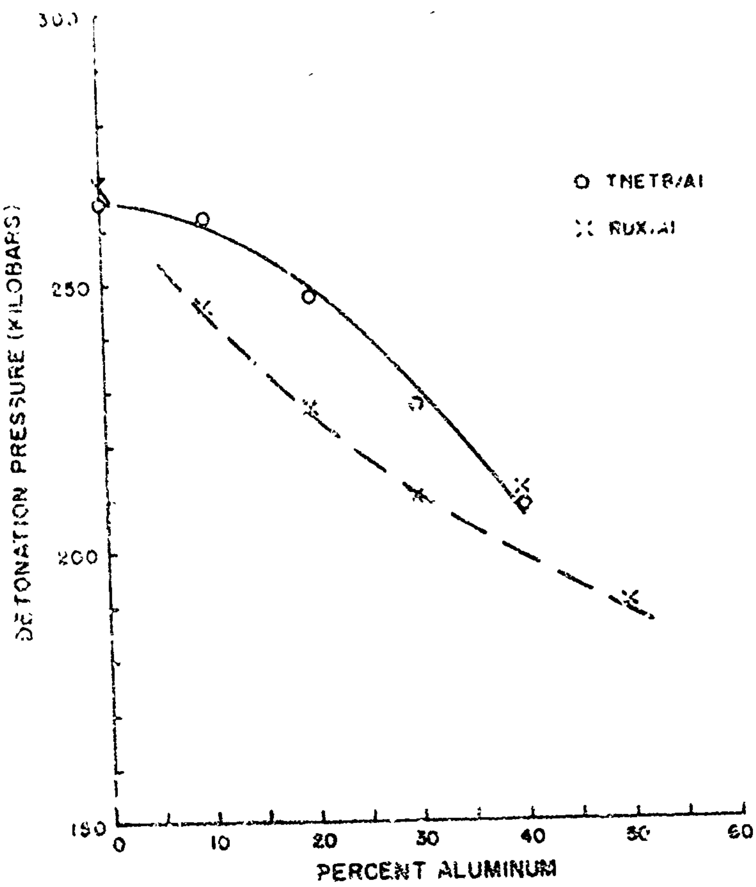

FIG 7 DETONATION PRESSURES OF TNETB/Al AND RDX/Al AS A FUNCTION OF THE PERCENT ALUMINUM

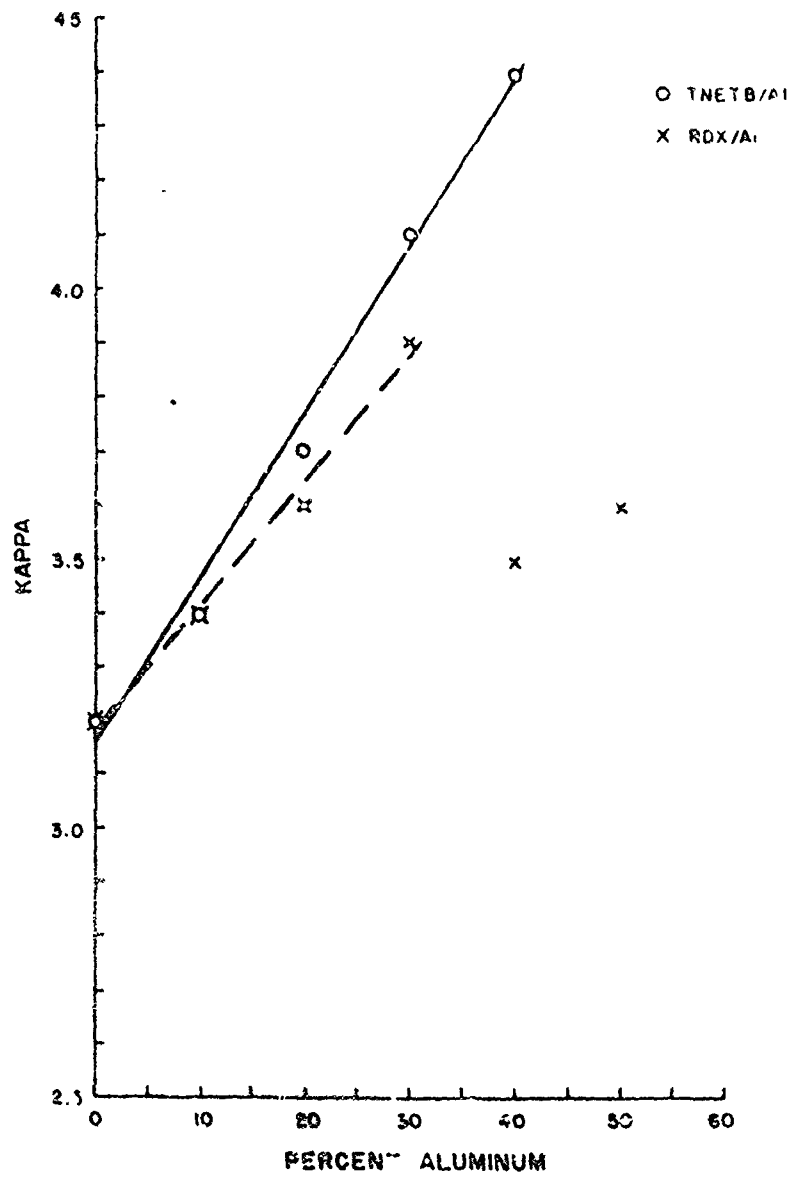

FIG.8 KAPPA VALUES OF RDX/Al AND TNETB/Al AS A FUNCTION OF THE PERCENT ALUMINUM

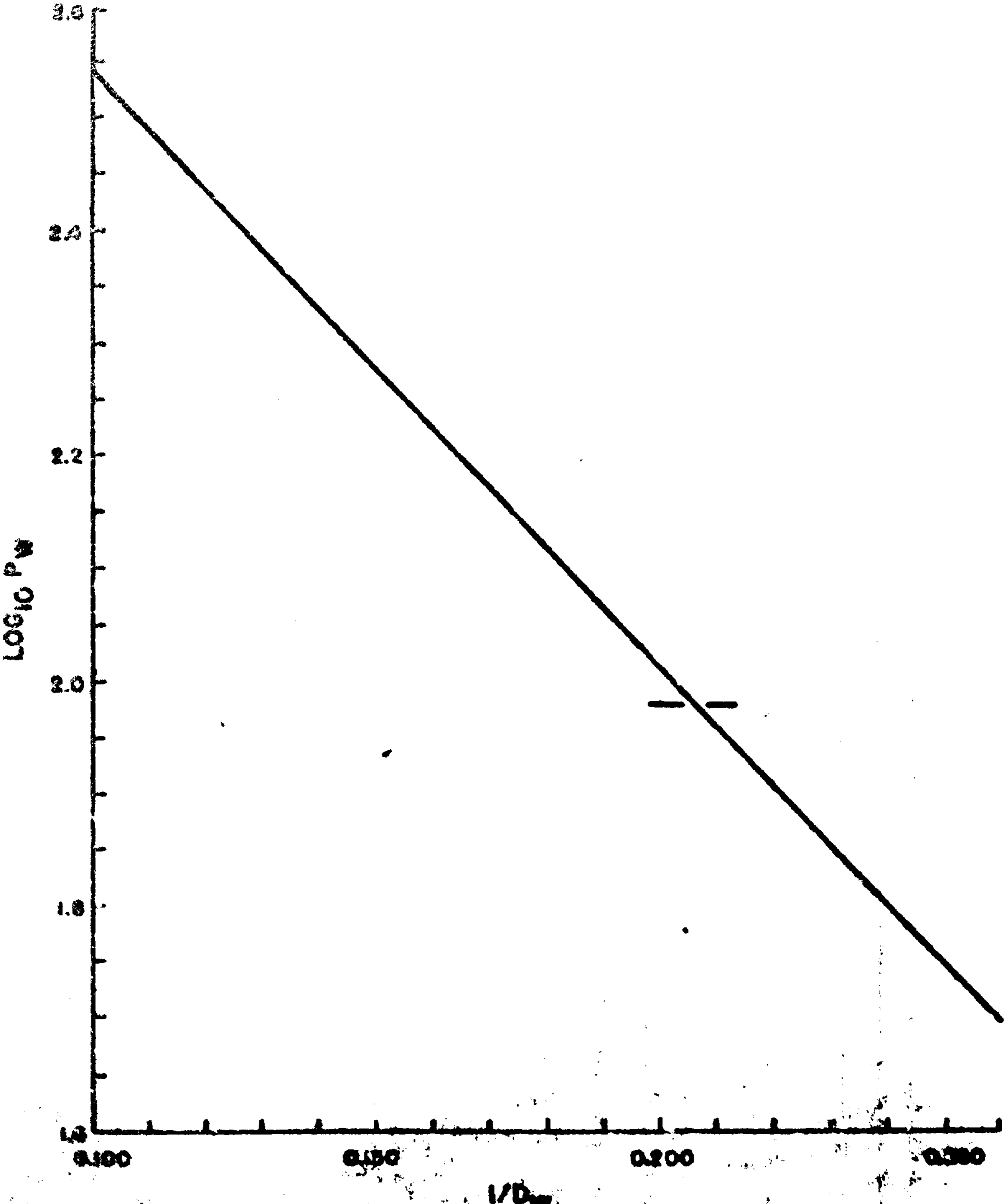

FIG. 9 LOG $P_W = 3.067 - 5.287 \times 1/D_W$. EXTRAPOLATED FROM SNAY AND R[illegible], NAVORD 23[illegible]

REFERENCES

(1) H. G. Snay and J. H. Rosenbaum, "Shock Wave Parameters in Fresh Water for Pressures Up to 95 Kilobars", NavOrd 2383.

(2) T. P. Liddiard and N. L. Coleburn; "The Addition of Aluminum to Various Explosives", to be published.

(3) H. Dean Mallory, "The Measurement of Detonation Pressures in Cast TNT", NavOrd 2913.

(4) R. D. Drosd, "A Gated Multiple Light Pulse Generator", NavOrd 3928.

(5) E. M. Boggs, "Conference on Temperature and Pressure of Detonation" NavOrd 84-46, July 1946.

(6) R. Schall, "Examination of X-Ray Flash Photographs on Detonation Waves", OTIB 1128, 14 March 1944.